

## Correlation functions in the two-dimensional random-bond Ising model

S. L. A. de Queiroz<sup>1,\*</sup> and R. B. Stinchcombe<sup>2,†</sup>

<sup>1</sup>*Instituto de Física, Universidade Federal Fluminense, Avenida Litorânea s/n, Campus da Praia Vermelha, 24210-340 Niterói, Rio de Janeiro, Brazil*

<sup>2</sup>*Theoretical Physics, Department of Physics, University of Oxford, 1 Keble Road, Oxford OX1 3NP, United Kingdom*  
(Received 4 March 1996)

We consider long strips of finite width  $L \leq 13$  sites of ferromagnetic Ising spins with random couplings distributed according to the binary distribution  $P(J_{ij}) = 1/2[\delta(J_{ij} - J_0) + \delta(J_{ij} - rJ_0)]$ ,  $0 < r < 1$ . Spin-spin correlation functions  $\langle \sigma_0 \sigma_R \rangle$  along the “infinite” direction are computed by transfer-matrix methods, at the critical temperature of the corresponding two-dimensional system, and their probability distribution is investigated. We show that, although in-sample fluctuations do not die out as strip length is increased, averaged values converge satisfactorily. These latter are very close to the critical correlation functions of the pure Ising model, in agreement with recent Monte Carlo simulations. A scaling approach is formulated, which provides the essential aspects of the  $R$  and  $L$  dependence of the probability distribution of  $\ln \langle \sigma_0 \sigma_R \rangle$ , including the result that the appropriate scaling variable is  $R/L$ . Predictions from scaling theory are borne out by numerical data, which show the probability distribution of  $\ln \langle \sigma_0 \sigma_R \rangle$  to be remarkably skewed at short distances, approaching a Gaussian only as  $R/L \gg 1$ . [S1063-651X(96)08506-6]

PACS number(s): 05.50.+q, 05.70.Jk, 64.60.Fr, 75.10.Nr

### I. INTRODUCTION

Most studies of random magnetic systems focus on whether or not quenched disorder destroys a sharp phase transition and, in the latter case, whether critical exponents are the same as for the corresponding pure magnets [1–3]. Less attention has been paid to the underlying probability distribution functions which govern the behavior of sample-averaged thermodynamic quantities, and which are expected to be universal in certain circumstances (see below). Early work on probability distributions of correlation functions concentrated, as numerical applications were concerned, on strictly one-dimensional systems [4–7]. The behavior, under renormalization group transformations, of the distribution of, e.g., conductivities in percolation-resistor networks [8], or interactions in spin glasses [9], has been studied as well. More recently, the probability distributions of bulk quantities such as energy, magnetization, specific heat, and susceptibility of disordered Ashkin-Teller models have been investigated in two dimensions [10] by Monte Carlo simulations. Bond distribution functions in one-dimensional quantum spin systems have been revisited very recently [11].

Here we deal directly with spin-spin correlation functions on finite-width strips of two-dimensional disordered Ising systems. The basic motivation for using this geometry is the fact that strip calculations, in conjunction with finite-size scaling concepts [12,13] are among the most accurate techniques to extract critical points and exponents for nonrandom low-dimensional systems [14,15]. The rate of decay of correlation functions determines correlation lengths along the strip. These latter are, in turn, a key piece of Nightingale’s phenomenological renormalization scheme [14,15], and have been given further relevance via the connection with critical

exponents provided by conformal invariance concepts [16]. Early extensions of strip scaling to random systems [17] have since been pursued further [18–20] and put into a broader perspective. Though this has been done with the help of ideas arising from the study of probability distributions [4–7], the behavior of the probability distributions themselves has not been closely investigated in strip geometries. In particular, their evolution toward the two-dimensional system’s form as strip width increases has not been analyzed to our knowledge.

We consider a two-dimensional random-bond Ising model on a square lattice with a binary distribution of ferromagnetic interaction strengths, each occurring with equal probability:

$$P(J_{ij}) = \frac{1}{2} [\delta(J_{ij} - J_0) + \delta(J_{ij} - rJ_0)], \quad 0 \leq r \leq 1. \quad (1)$$

For this case, the transition temperature  $\beta_c = 1/k_B T_c$  is exactly known from duality [21,22],

$$\sinh(2\beta_c J_0) \sinh(2\beta_c r J_0) = 1. \quad (2)$$

We have studied strips of width  $L \leq 13$  sites, with periodic boundary conditions, and length  $N = 10^6$  sites. Throughout this work we fix  $r = 1/4$  and  $T = T_c(1/4)$  as given by Eq. (2). Numerically,  $T_c(1/4)/J_0 = 1.239\dots$  [to be compared with  $T_c(1)/J_0 = 2.269\dots$ ]. Using this value of  $r$  ensures that disorder effects are rather strong, while at the same time one keeps a safe distance from the percolation regime at  $r = 0$  (near which crossover to geometry-dominated behavior is expected to complicate the picture); this choice also coincides with that used in several recent Monte Carlo simulations [3,23]; thus comparison (when appropriate) is made easier. The choice of  $T = T_c$  is important, as it is here that the probability distributions are expected to have a nontrivial universal form; furthermore, the extensive literature on critical correlations for pure systems, both making explicit connection to conformal invariance ideas [16] and previous to

\*Electronic address: sldq@if.uff.br

†Electronic address: stinch@thphys.ox.ac.uk

that (see, e.g., Ref. [24] and references therein), is an important reference frame against which to set our results.

In what follows, we first illustrate the role played by intrinsic fluctuations in the probability distribution of correlation functions, and show that even though these do not die away for large samples, the sample-to-sample fluctuations of averaged values do go down as sample size increases. Next we compare our results for averaged critical correlations with those for a pure system, in order to check on a recent proposal arising from Monte Carlo data [23] which implies equality, within error bars, of the corresponding quantities. We then go on to identify the key features of the shape of distributions, and investigate their variation with distance  $R$  and strip width  $L$ . A simplified scaling theory is formulated, which provides the essential aspects of the  $R$  and  $L$  dependence. Numerical data for the probability distributions of correlation functions bear out the main predictions of scaling theory, in particular the role played by the combination  $R/L$  as an appropriate scaling variable.

## II. INTRINSIC FLUCTUATIONS AND AVERAGES

We calculate the spin-spin correlation function  $G(R) \equiv \langle \sigma_0^1 \sigma_R^1 \rangle$ , between spins on the same row (say, row 1), and  $R$  columns apart, of strips with periodic boundary conditions along the vertical direction. This is done following the lines of Sec. 1.4 of Ref. [15], with standard adaptations for an inhomogeneous system [19]. At each iteration of the transfer matrix from one column to the next, the respective vertical and horizontal bonds between first-neighbor spins are drawn from the bond probability distribution, Eq. (1). By shifting the origin along the strip and accumulating the corresponding results, one then obtains averages of the correlation function (or of any function  $F$  of it, such as its logarithm, which will be of particular importance in what follows), to be denoted by  $\langle G \rangle$  [or  $\langle F(G) \rangle$ ], the  $R$  dependence being implicitly understood. With strips of length  $N=10^6$  sites, we are able to produce  $10^4$ – $10^5$  independent estimates of  $G$  for  $7 \leq R \leq 100$ , which is the range of distances to concern us here.

Normalized histograms of occurrence of the allowed values of the correlation function (or, rather more frequent below, of its logarithm) are produced by dividing a convenient interval of variation of  $G$  (or  $\ln G$ ) into  $10^3$  equal-width bins, and assigning each particular realization to the appropriate bin. For  $\ln G$  the interval ranging from  $\ln 10^{-7}$  to zero has proved generally adequate, except for  $R=100$ , where the lower limit was pushed down to  $\ln 10^{-11}$ .

For strictly one-dimensional disordered systems (i.e., chains) the average free energy (related to the largest Lyapunov exponent) has a normal distribution [4,5,7], as befits a sum of random variables. Thus the fluctuations shrink with sample size (strip length)  $N$ , and relative errors must die out as  $1/\sqrt{N}$ . Correlation functions, on the other hand, are products of random variables, thus their distribution tends to a log-normal form as  $R \rightarrow \infty$  [4], that is, the probability distribution of  $\ln G$  approaches a Gaussian. However, the analysis of correlation functions turns out to be more complex than that of the free energy, even on chains; a primary reason for this is that while the latter quantity is self-averaging in the sense defined above, the former is not: the usual Brout

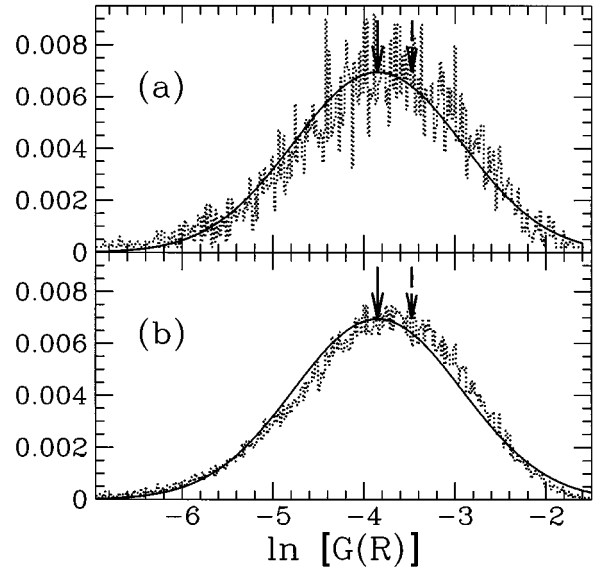


FIG. 1. Normalized histograms of occurrence of  $\ln G$  for  $L=5$ ,  $R=20$ . (a)  $N=10^5$ ; (b)  $N=10^6$ . Full vertical arrows at  $\langle \ln G \rangle$ ; broken vertical arrows at  $\Delta \langle \ln G \rangle$ . Curves are Gaussians fitted to mean and root-mean-square deviation of  $\ln G$ , as calculated from respective realizations. Here, and in all subsequent figures,  $r=1/4$  and  $T=T_c(r)$ .

argument [25] cannot be applied, as explained, e.g., in Ref. [5]. The width of the probability distribution of correlation functions is then expected to be a permanent feature, which will not vanish (at least trivially) with increasing sample size.

We have found that on finite-width strips the width of the distribution tends to stay essentially constant as  $N$  varies. A graphic illustration is provided in Fig. 1, where the horizontal variable is  $\ln G$ , which turns out to be convenient for most purposes (see below). Increasing  $N$  simply smooths out the histogram; averages such as  $\langle G \rangle$  or  $\langle \ln G \rangle$  hardly move, the same being true of the width. This is easier to notice by comparing the Gaussians fitted to peak at  $\langle \ln G \rangle$  and with width given by the root-mean-square deviation  $\Delta(\ln G) \equiv \{ \langle [\ln G - \langle \ln G \rangle]^2 \rangle \}^{1/2}$ .

Though neither  $\Delta(\ln G)$  or  $\Delta G$  vanishes, it is still possible to extract valuable information from averaged values, the dispersion of which among independent samples (to be denoted, respectively,  $\Delta \langle \ln G \rangle$  or  $\Delta \langle G \rangle$ ) does shrink with increasing sample size. Figure 2 shows the typical dependence of relative fluctuations,  $\Delta G / \langle G \rangle$  and  $\Delta \langle G \rangle / \langle G \rangle$ , with strip length  $N$ . Varying the number  $n$  of distinct (that is,  $N$  lattice spacings long) samples within a reasonable interval, say  $n=5$ – $50$ , changes  $\Delta \langle G \rangle$  only slightly, consistent with a  $1/\sqrt{n}$  dependence to be inferred from standard arguments. From an investigation of  $\Delta \langle G \rangle / \langle G \rangle$  for distances in the range  $R=7$ – $50$  and strip widths up to  $L=7$ , it turns out that both the order of magnitude and  $N$  dependence (roughly  $1/\sqrt{N}$ ) depicted in Fig. 2 are typical. The behavior of  $\Delta \langle \ln G \rangle / \langle \ln G \rangle$  is entirely similar. We can thus predict (see Fig. 2) that the fluctuations  $\Delta \langle \ln G \rangle / \langle \ln G \rangle$  and  $\Delta \langle G \rangle / \langle G \rangle$  will be of order 1% or just under that for strips of length  $N=10^6$ . This will be enough for our purposes here. Similar considerations have been used elsewhere in strip studies [20], and seem to have been followed also in Monte Carlo

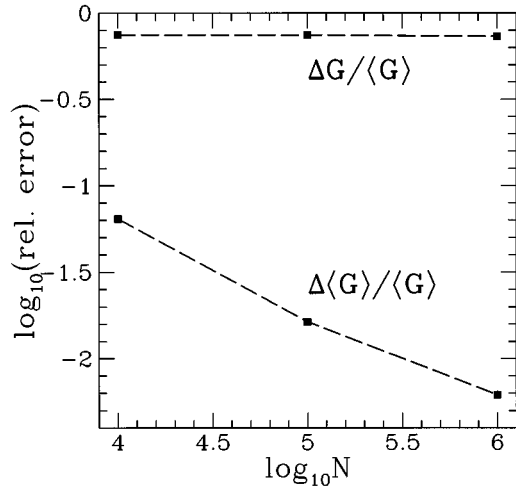


FIG. 2. Relative fluctuations within sample,  $\Delta G/\langle G \rangle$ , and between sample-averaged values,  $\Delta \langle G \rangle/\langle G \rangle$ , against strip length  $N$ .  $L=7$ ,  $R=20$ , number of samples  $n=20$ .

calculations of correlation functions in finite ( $L \times L$ ) systems [23].

### III. COMPARISON WITH PURE-SYSTEM CRITICAL CORRELATIONS

It has been found in Monte Carlo simulations [23] that the average correlation function at criticality of a random-bond Ising system is numerically very close to that for a pure system at its own critical point. Below we check on the corresponding quantities for the strip geometry.

The spin-spin correlation function for the pure Ising model at  $T=T_c$  on a strip of width  $L$  is known from conformal invariance [16] to vary, for large  $R$ ,  $L$  as

$$\langle \sigma_0^1 \sigma_R^1 \rangle \sim \left( \frac{\pi/L}{\sinh(\pi R/L)} \right)^\eta, \quad \eta=1/4, \quad (3)$$

for spins along the same row as is the case here. The proportionality factor can be obtained from the exact square-lattice ( $L \rightarrow \infty$ ) result [24],  $\langle \sigma_0^1 \sigma_R^1 \rangle = 0.70338/R^{1/4}$ . In Fig. 3 we show, for  $R=7$  and 20, data for  $\langle G \rangle$  and  $\exp\langle \ln G \rangle$  together with a continuous curve for the pure system. The latter passes through numerically calculated points for  $L \leq 15$  [Eq. (3) is in error by one part in  $10^4$  for  $L=15$ ,  $R=7$  and less than that for  $R=20$ ] and follows Eq. (3) for larger  $L$ . Using  $1/L^2$  for the horizontal axis guarantees that the pure-system curve approaches the vertical axis linearly. However, it still shows high curvature even for the largest values of  $L$  attainable in our random-system calculations. This warns us to refrain from extrapolating our data for  $L \rightarrow \infty$ . Even so, we can learn from finite-width results that  $\langle G \rangle$  behaves very closely to its pure-system counterpart. This is in line with previous findings [19] according to which in a random system the correlation length  $\xi$  to be used in the exponent-amplitude relation of conformal invariance,  $\xi=L/\pi\eta$  [16], is that obtained from the average decay of  $\langle G \rangle$  against  $R$ . Thus one gets a picture in which  $\eta=1/4$  as for the pure system [19], consistent with  $\gamma/\nu=7/4$  obtained, e.g., from strip calculations of the average susceptibility for the random system [20], and the scaling relation  $\gamma/\nu=2-\eta$ .

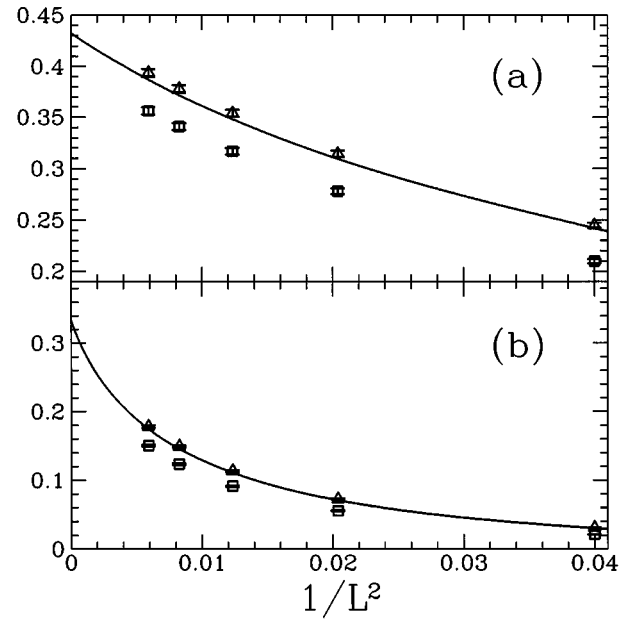


FIG. 3. Averaged correlation functions for  $L=5, 7, 9, 11, 13$ . (a)  $R=7$ ; (b)  $R=20$ . Triangles:  $\langle G \rangle$ ; squares:  $\exp\langle \ln G \rangle$ . Errors as defined in Sec. II. Continuous line: correlation functions for pure Ising model on strips [16,24].

Of course the present result reaches further, as one could conceive of a scenario where the correlations would differ in the pure and random systems, but decay asymptotically as  $R \rightarrow \infty$  with the same rate (thus giving the same  $\xi$ ). In fact, the decay of  $\exp\langle \ln G \rangle$  against  $R$  is not too dissimilar to that of  $\langle G \rangle$  for moderate disorder, and for the finite values of  $L$  within reach of calculation. Only a systematic study of extrapolation trends as  $L \rightarrow \infty$ , covering different degrees of disorder, shows how the respective correlation lengths are essentially distinct [19]. The physical origin of this lies in that, on account of the properties of the probability distribution of  $G$  (to be seen in detail below), the most probable value  $\exp\langle \ln G \rangle$  does not coincide with the average one,  $\langle G \rangle$  [6,7]. Accordingly, it has been shown by field-theoretic arguments [26] and supported by numerical work [19] that the most probable, or typical, correlation function decays as

$$\exp\langle \ln G \rangle \sim R^{-1/4} (\ln R)^{-1/8}, \quad (4)$$

while the logarithmic corrections are washed away upon averaging for  $\langle G \rangle$ , resulting in a purely algebraic decay with  $\eta=1/4$ .

Quantitative analysis of the results displayed in Fig. 3 shows that, considering the central estimates  $\langle G \rangle$  the ratio  $Q \equiv \langle G(R, L, r, T_c(r)) \rangle / \langle G(R, L, 1, T_c(1)) \rangle$  is, in all cases, within 1.01–1.03. With estimated error bars of order 1% as explained in the preceding section, a very small amount of overshooting seems to persist which does not follow a definite trend against  $R/L$  (see Fig. 4). Monte Carlo data show the corresponding ratio approaching unity from below as lattice size  $L$  increases [23], in the region  $R/L \ll 1$ . We cannot go far into that region, as the maximum strip widths within reach are not much larger than 10, and randomness effects are significantly distorted for small  $R \leq 5$ .

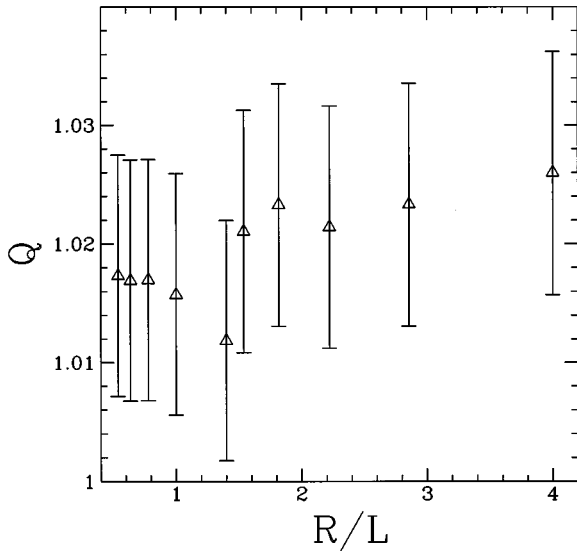


FIG. 4. Ratio  $Q \equiv \langle G(R, L, r, T_c(r)) \rangle / G(R, L, 1, T_c(1))$  against  $R/L$  for points of Fig. 3. Error bars represent estimated fluctuations of order 1%.

Though we are not able at this point to advance a quantitative argument, it is plausible that finite-size effects manifest themselves differently in strip and square geometries; taken together with those of Ref. [23], we interpret our data as evidence in favour of pure- and random-system critical correlations being in fact equal, at least for  $R, L \gg 1$  and  $R/L \leq 1$ .

In the next two sections, we exploit the features of the probability distribution of  $G$ , and show that the variable  $R/L$  is indeed at least approximately the convenient one to describe several relevant aspects of the problem.

#### IV. PROBABILITY DISTRIBUTIONS: SCALING THEORY

##### A. Relevant parameters

Our starting point is the result that, in one dimension and for large  $R$  the probability distribution of  $G$  must be log-normal [4–7]. The same is expected to hold on strips provided that  $R/L \gg 1$ . We seek for deviations from Gaussian behavior as one moves away from this limit.

In Fig. 5 we show normalized histograms of occurrence of  $\ln G$  for fixed  $L=5$  and  $R=7, 20$  and  $50$ . Though to zeroth order one could say that all plots look similar to Gaussians, the semblance is reduced as  $R$  decreases.

A quantitative measure of departure from Gaussian behavior is the (dimensionless) skewness  $S$ , defined as [27]

$$S \equiv \left( \frac{\langle x - \langle x \rangle \rangle^3}{\sigma} \right)^3 \quad (5)$$

for a distribution with mean  $\langle x \rangle$  and dispersion  $\sigma$ . Of course, for a finite number of realizations of a given probability distribution  $S$  itself will be subject to fluctuations. In what follows we shall always quote  $S$  with two significant digits, which will allow us to discern trends while staying reasonably within reliable margins. For  $L=5$  and  $R=7, 20, 50$  and  $100$  (the latter not shown in Fig. 5) one has, respectively,  $S = -0.67, -0.41, -0.24$ , and  $-0.19$ . We shall analyze the

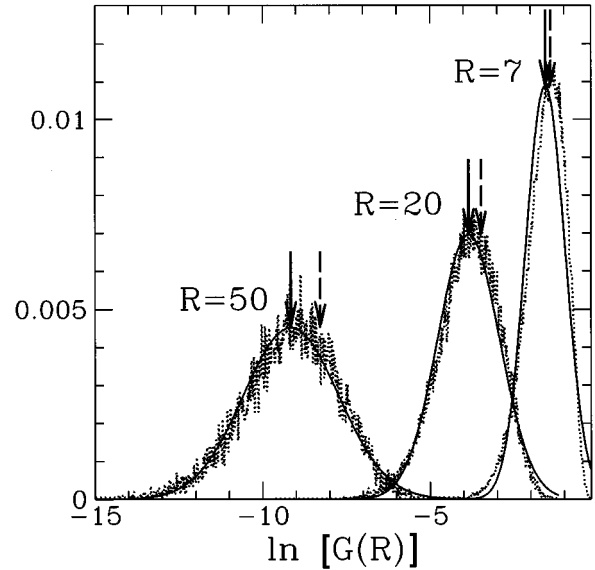


FIG. 5. Normalized histograms of occurrence of  $\ln G$  for fixed  $L=5$  and  $R=7, 20$  and  $50$ . Full vertical arrows at  $\langle \ln G \rangle$ ; broken vertical arrows at  $\Delta \langle \ln G \rangle$ . Curves are Gaussians fitted to mean and root-mean-square deviation of  $\ln G$ , as calculated from respective realizations.

$R$  and  $L$  dependence of  $S$  below; for the moment note that it approaches zero with increasing  $R$ , as expected, and is always negative. This is partly because of the many-channel, incipiently two-dimensional character of correlations on the strip: qualitatively, if there is at least one path of “strong” bonds between two spins, their correlation is significant, and is not much enhanced if there are more strong-bond paths, thus the peak at large  $\ln G$  with an abrupt cutoff above the maximum; on the other hand, configurations without any strong-bond paths at all are possible but with low probability, giving rise to the “tail” of very low  $\ln G$  values. This argument explains the general trend towards increasing  $|S|$  for  $R/L < 1$  as well (see below). An extreme example of this trend is shown in Fig. 6 for  $L=13, R=7$  where  $S = -0.85$ . The negative skewness effect depends also on the variable against which histograms are plotted: here we use  $\ln G$  because our goal is to check on departures from a log-normal distribution, thus it is the skewness of this plot which matters in the context. For instance, a plot of the same distribution against  $\tanh^{-1} G$  would have positive skewness.

We choose to characterize the distribution of  $\ln G$  by three quantities, namely, mean ( $\langle \ln G \rangle$ ), dispersion, or root-mean-square deviation [ $\Delta(\ln G)$ ] and skewness ( $S$ ). In other words, we assume that the probability distribution of correlation functions is satisfactorily described by perturbative corrections to a log-normal form. As shown below, this works well in the present case of ferromagnetic disorder. If frustration effects are present, such as, e.g., in random-field [28] or spin-glass systems, it may be necessary to take recourse to additional parameters, or even to adopt a different perspective. We shall not deal with this matter in the present work.

##### B. Scaling theory

The aspects just described are consistent with a scaling description given in this section. It leads to further specific

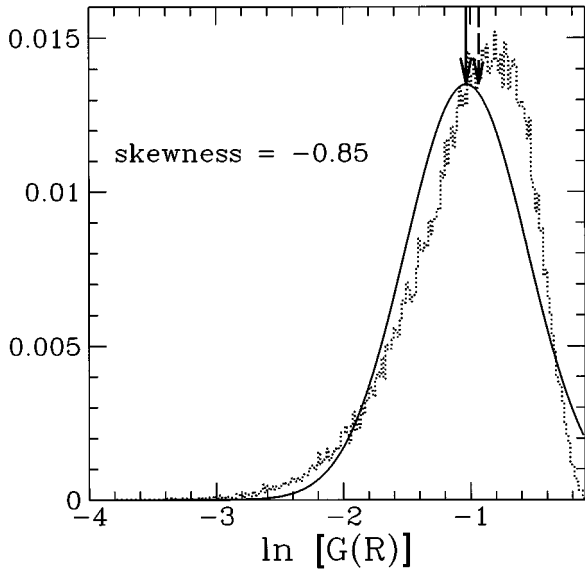


FIG. 6. Normalized histogram of occurrence of  $\ln G$  for  $L=13$  and  $R=7$ . Full vertical arrow at  $\langle \ln G \rangle$ ; broken vertical arrow at  $\ln(G)$ . Curve is Gaussian fitted to mean and root-mean-square deviation of  $\ln G$ , as calculated from respective realization. Skewness  $= -0.85$ .

predictions regarding the form of distribution functions and their dependences on the variables  $R$  and  $L$ , which will be discussed subsequently in the light of the numerical results.

The approach combines two main features: (i) the appearance at large scales  $L, R \gg 1$  of universal aspects related to fixed point Hamiltonian and probability distributions of the disordered two-dimensional (2D) Ising model; and (ii) the crossover for  $R > L$  to width-limited behavior characteristic of the one-dimensional (1D) version of the large-scale universal properties.

The procedure is to first scale  $n$  times by (length) rescaling factor  $b$ , where  $b^n = L$ , which takes the system to an equivalent linear chain. This step involves the scaling of joint probability distributions for the appropriate variables. If one starts from the critical condition of the random 2D Ising system irrelevant variables scale away, and one approaches asymptotically the fixed point Hamiltonian and distribution describing the universality class containing the 2D random Ising system. This involves a minimal set of relevant random variables  $\{t_i^{(n)}\}$  (after  $n$  scalings) and their universal probability distributions. The correlation function scales as follows:

$$\begin{aligned} G_L(R, \{t_i\}) &= b^{-\eta} G_{L/b}(R/b, \{t_i^{(1)}\}) \\ &= \dots = L^{-\eta} G_1(R/L, \{t_i^{(n)}\}) \quad (n = \ln L / \ln b). \end{aligned} \quad (6)$$

We now have an equivalent 1D system with Hamiltonian close to the fixed point Hamiltonian of the disordered 2D system. Since the correlations in a 1D system are transmitted through each intermediate space point, a factorization of  $G_1(R/L, \{t_i^{(n)}\})$  is suggested if  $R/L > 1$ . This factorization is into  $R/L$  factors corresponding to successive  $L \times L$  blocks of the original system (i.e., to single bonds of the renormalized 1D system), labeled by  $s = 1, \dots, R/L$ ; then Eq. (6) becomes

$$G_L(R, \{t_{ij}\}) = L^{-\eta} \prod_{s=1}^{R/L} G_1(1, \{t_i^{(n)}\}_s). \quad (7)$$

Here,  $\{t_i^{(n)}\}_s$  are the renormalized random variables for the block labeled by  $s$ . It will be assumed later that these are largely uncorrelated from one block  $s$  to another, since the blocks were initially nonoverlapping. This, and the other approximations leading to the approximate form Eq. (7) will be tested by later comparison to the numerical results. Equation (7) generalizes a result for the pure case. There, for  $R/L$  large,  $G_1(R/L, \dots, t^* \dots) \propto (\lambda_2/\lambda_1)^{R/L}$ , where  $\lambda_2/\lambda_1$  is a universal ratio of eigenvalues of the transfer matrix of the universal fixed point Hamiltonian of the pure 2D Ising class. Then

$$G_L(R, t^*) \propto L^{-\eta} \exp[-R/\xi_L], \quad (8)$$

where  $\xi_L^{-1} = 1/L \ln(\lambda_1/\lambda_2)$  ( $= \pi\eta/L$  [16]). It is perhaps interesting that the simplest  $b=2$  Migdal-Kadanoff real-space renormalization group transformation gives  $G_1(R/L, t^*) = (t^*)^{R/L}$ ,  $t^* = 0.544$ , hence it gives  $\eta \sim 0.19$ . This unsatisfactory representation of the universal  $\eta$  in terms of a nonuniversal  $t^*$  is due to not having allowed the Hamiltonian to adopt its universal form.

We now return to the disordered case and consider the development of the probability distributions during the rescalings leading to Eq. (6). To allow for correlations it is necessary to consider the probability distribution  $P_{\{t_{ij}\}}$  for the whole set of  $t_i$ 's. This is labeled by a parameter  $t$  setting the scale for all the  $t_i$ 's. The scaling of the distribution is given by a mapping  $W_b$ :

$$P_{t^{(l+1)}}^{(l+1)}\{\{t_{ij}\}\} = W_b\{P_{t^{(l)}}^{(l)}\{\{t_{ij}\}\}\} = W_b^l\{P_{t^{(0)}}^{(0)}\{\{t_{ij}\}\}\}, \quad (9)$$

where  $l, l+1$  label two successive steps, and  $W_b^l$  denotes  $l$  iterations of the map. The parameter  $t$  also scales according to a renormalization group transformation characteristic of the 2D random Ising model. At the fixed point  $t^*$  of that transformation, after  $n = \ln L / \ln b$  scalings with  $n$  large,  $W_b^n$  will have produced a distribution  $P_{t^*}^{(n)}$  close to the universal invariant distribution  $P_{t^*}^*$  of the random 2D Ising model, which satisfies the fixed point equation

$$P_{t^*}^*\{\{t_{ij}\}\} = W_b\{P_{t^*}^*\{\{t_{ij}\}\}\}. \quad (10)$$

Then, employing Eq. (7) and taking logarithms to obtain a sum of random variables on the right-hand side we find that at  $t^*$ , after  $n$  scalings, the probability distribution  $\mathcal{A}(\alpha)$  for  $\ln G_L$  [i.e., for the probability that  $\ln G_L(R, \{t_{ij}\})$  takes the value  $\alpha$ ] is given by

$$\begin{aligned} & \int d\alpha \exp(\beta\alpha) \mathcal{A}(\alpha) \\ &= \int \left( \prod dt_i \right) P_{t^*}^{(n)}\{\{t_{ij}\}\} \\ & \quad \times \exp(-\beta\eta \ln L) \prod_{s=1}^{R/L} \exp[\beta \ln G_1(1, \{t_{ij}\}_s)]. \end{aligned} \quad (11)$$

If  $n$  is large, as well as  $P_{t^*}^{(n)} \sim P_{t^*}^*$ , we have  $G_1(1, \{t_{ij}\}_s)$  close to a universal function characteristic of the random 2D Ising class, since the renormalized bond regions labeled by each  $s$  are each a composition of many original bonds, at  $t^*$ .

To the extent that the probability distribution  $P_{t^*}^{(n)}$  factorizes into parts  $q_{t^*}^{(n)}\{t_{ij}\}_s$  corresponding to the different  $s$ 's (to be tested) the result Eq. (11) reduces to a form corresponding to the probability of a sum of random variables ( $\ln G_1$ ):

$$\int d\alpha \exp(\beta\alpha) \mathcal{A}(\alpha) = \exp(-\beta\eta \ln L) [I^{(n)}(\beta)]^{R/L}, \quad (12)$$

with

$$I^{(n)}(\beta) = \int \left( \prod dt_i \right) q_{t^*}^{(n)}\{t_{ij}\}_s \exp[\beta \ln G_1(1, \{t_{ij}\}_s)], \quad (13)$$

where the subscript  $s$  indicates that all  $t_i$ 's are in the region corresponding to a given  $s$ .

We now explore the consequences of the above results, and in particular the expected universality of  $q_{t^*}^{(n)}$ ,  $G_1(1, \{t_{ij}\}_s)$  for  $L (=b^n)$  large, for the distribution  $\mathcal{A}(\alpha)$  for  $\ln G_L(R, \{t_{ij}\}_s)$ .

Equation (12) shows that  $\mathcal{A}(\alpha - \eta \ln L)$  corresponds to the probability distribution for a sum of  $R/L$  independent random variables [ $\ln G_1(1, \{t_{ij}\}_s)$ ], and has the consequence that, if  $R/L$  is large,  $\mathcal{A}(\alpha)$  approaches a Gaussian distribution with mean, width, and skewness given by

$$\langle \alpha \rangle = \left( \frac{R}{L} \right) m - \eta \ln L, \quad (14)$$

$$\langle (\alpha - \langle \alpha \rangle)^2 \rangle^{1/2} = \left( \frac{R}{L} \right)^{1/2} w, \quad (15)$$

$$\langle (\alpha - \langle \alpha \rangle)^3 \rangle / \langle (\alpha - \langle \alpha \rangle)^2 \rangle^{3/2} = \left( \frac{R}{L} \right)^{-1/2} s. \quad (16)$$

The quantities  $m$ ,  $w$ , and  $s$  are characteristics of  $I^{(n)}(\beta)$ , which is related as follows to the (non-Gaussian) distribution function  $Q^{(n)}(\alpha)$  for the logarithm of the nearest-neighbor correlation function of the ( $n$ -times rescaled) disordered 2D Ising system:

$$I^{(n)}(\beta) = \int d\alpha \exp(\beta\alpha) Q_1^{(n)}(\alpha), \quad (17)$$

with

$$Q_1^{(n)}(\alpha) = \int \left( \prod dt_i \right) q_{t^*}^{(n)}\{t_{ij}\}_s \delta(\alpha - \ln G_1(1, \{t_{ij}\}_s)). \quad (18)$$

For  $L = b^n$  large, all these quantities and therefore  $m$ ,  $w$ , and  $s$  will become universal (characteristic of the 2D random Ising class).

The universal character at large  $L$  of the distribution  $\mathcal{A}(\alpha)$  for  $\ln G_L(R)$  at  $t^*$ , its Gaussian form at large  $R/L$ , and the results (14)–(16) and their interpretation above, are the main

conclusions of this section. Note (a) that these conclusions include the result of Ref. [4] for the 1D case and (b) that the analogue of  $m$  for the pure case is the universal constant  $-\pi\eta$  (while  $w$ ,  $s$  are zero).

The essential points of the general discussion given above can be explicitly illustrated in the simple scenario provided by the renormalization group approach (blocking-decimation), allowing for just the random variables  $\{t_i \equiv \tanh \beta J_i\}$ . This forces the Hamiltonian to remain of Ising form [so the rescaling expressed under Eq. (8) applies]. We allow for spin rescaling, and for the distribution function  $g(t_i)$  for each  $t_i$  to develop towards fixed point universal form under the scaling [8,9], but we ignore correlations. Then  $G_1(1, \{t_i\})$  is just the renormalized variable  $t_i^{(n)}$ . The scaling of  $t_i$  will be of the form

$$t_i^{(l+1)} = R_b \{t_i^{(l)}\}, \quad (19)$$

where the right-hand side is a function of  $N_b$  variables  $t_i^{(l)}$  comprising the block. Then the distribution  $g^{(l)}(t_i^{(l)})$  scales according to the following simplified version of Eq. (9):

$$g_{t^{(l+1)}}^{(l+1)}(t') = \int \left( \prod_{i=1}^{N_b} dt_i g_{t^{(l)}}^{(l)}(t_i) \right) \delta(t' - R_b \{t_i^{(l)}\}), \quad (20)$$

and  $t^{(l)} \rightarrow t^{(l+1)}$  is the resulting change of scale of the distribution  $g$ . No scale change occurs if the initial distribution is set at the critical value of  $t^{(0)}$ . Then, for large  $l$ , Eq. (20) gives the asymptotic approach to the universal fixed point distribution, from which  $m$ ,  $w$ ,  $s$  can be obtained. For an adequate description of this sort, the transformation Eq. (19) should give the proper zero value of the exponent  $\alpha$  for the pure case: via the Harris criterion this makes the disorder marginally relevant and ensures that the width  $w$  does not scale away. It requires  $N_b = \lambda_b^2$ , where  $\lambda_b = b^{1/\nu}$  is the eigenvalue of the pure version of Eq. (19), linearized about its fixed point. Procedures of this sort give (i)  $m$  not very different from its pure value; and (ii) negative skewness  $s$ .

## V. NUMERICAL RESULTS AND CONTACT WITH THE SCALING THEORY

We begin by recalling that the results exhibited in Fig. 2 point out the importance of intrinsic widths in the critical random system (i.e., at  $t^*$ ). This is a central feature of the scaling theory, through the appearance of universal distributions. Secondly, we recall that Fig. 5 provides evidence for Gaussian distributions for  $\ln G$  at large  $R$ , with narrowing relative widths as  $R$  increases. This is again a prediction of the scaling theory [see Eq. (14) and the discussion preceding it].

The results already presented in Fig. 3 show that the overall dependence of  $\exp(\ln G)$  on  $L$  for fixed  $R$  approximately mimics that of  $\langle G \rangle$ , apart from a proportionality factor. The latter is, in turn, numerically very close (see Fig. 4) to that of the pure system, given to good approximation by Eq. (3). The proportionality factor is, however,  $R$  dependent, as illustrated in Fig. 7; this illustrates that, though both quantities decay exponentially with  $R$  as befits an essentially one-dimensional system, their respective correlation lengths differ, with well-known consequences [6,7,19]. The linear de-

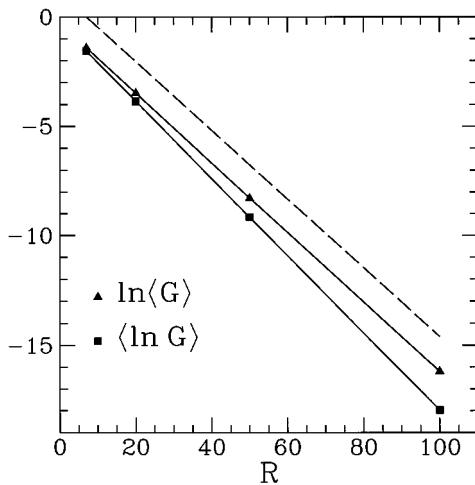


FIG. 7. Semilog plot of decay of  $\langle \ln G \rangle$  and  $\ln \langle G \rangle$  against distance for fixed  $L=5$ . Broken line gives slope as predicted by conformal invariance ( $L/\xi = \pi\eta$ ) with  $\eta=1/4$ .

pendence of  $\langle \ln G \rangle \equiv \alpha$  against  $R$  is consistent with the scaling result (14).

Also, at large  $R$ , the slope of the measured  $\alpha$  versus  $R$  line is proportional to  $1/L$ , in agreement with the  $(R/L)^m$  term dominant in Eq. (14); and the coefficient is consistent with having  $m$  not far from its pure value. The comparison of numerical results for  $\langle \ln G \rangle$  and  $\langle G \rangle$  with corresponding pure forms is given in Fig. 8, where  $G_{\text{pure}}$  is given by Eq. (3) above.

A further, rather stringent test of the scaling predictions is the plot in Fig. 9 of numerical data for  $\Delta(\ln G)$  against  $R/L$ . It can be seen that the  $(R/L)^{1/2}$  dependence Eq. (15) is reasonably followed in the large  $R/L$  regime where it was derived; and the data collapse of results for different  $R, L$  sug-

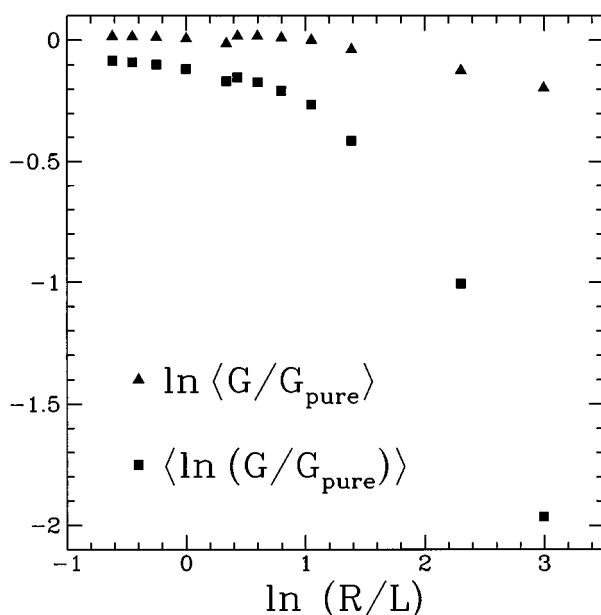


FIG. 8. Log-log plot of ratio between averaged correlation functions and  $G_{\text{pure}}$  against  $R/L$ , the latter as given in Fig. 3 [16,24]. Triangles: data from  $\langle G \rangle$ ; squares: data from  $\langle \ln G \rangle$ .

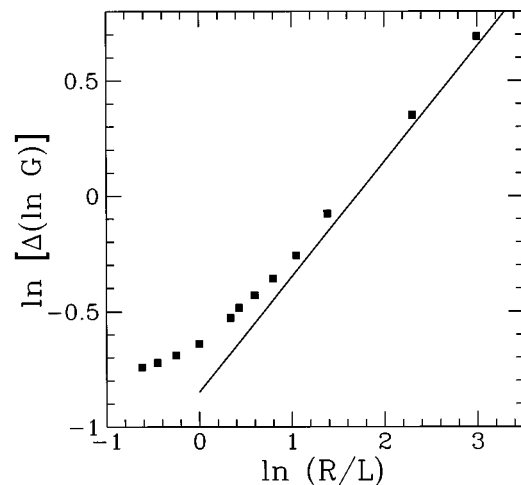


FIG. 9. Log-log plot of width  $\Delta(\ln G)$  against distance  $R/L$ . Line has slope  $1/2$ .

gests that  $R/L$  is (as predicted) the appropriate scaling variable in the regime of large  $R, L$  independent of their ratio. The curve also gives evidence of the crossover to the universal width of the 2D random Ising system for  $L \geq R \gg 1$ .

In order to further test the scaling theory, and the suggestion that  $R/L$  is the appropriate scaling variable, we show in Fig. 10 numerical results for the skewness against  $R/L$ . Again the data collapse is satisfactory. The prediction of  $(R/L)^{-1/2}$  behavior [Eq. (16)] for large  $R/L$  is again observed, and the crossover towards universal 2D behavior is seen for  $L \geq R \gg 1$ .

## VI. CONCLUSIONS

We have studied properties of the probability distributions of correlation functions on finite-width strips of the two-dimensional random-bond Ising model at criticality. We have shown that even though intrinsic fluctuations in the probability distribution do not die away for large samples, the sample-to-sample fluctuations of averaged values do go down approximately with the square root of sample size as

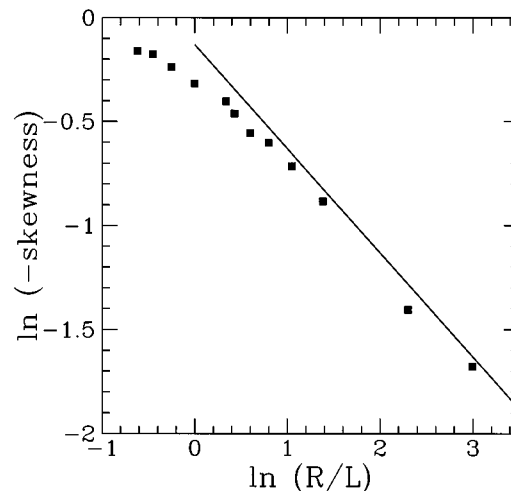


FIG. 10. Log-log plot of negative skewness  $-S$  against  $R/L$ . Line has slope  $-1/2$ .

the latter increases. Results thus obtained for averaged critical correlations have been compared with those for a pure system, and we have found that the values of averaged correlations  $\langle G \rangle$  are very close to the corresponding pure-system ones, consistent with recent Monte Carlo data [23]. The key features of the shape of distributions have been identified, and a simplified scaling theory has been formulated, which provides the essential aspects of the  $R$  and  $L$  dependence. Numerical data for the probability distributions of correlation functions bear out the main predictions of scaling theory, in particular the role played by the combination  $R/L$  as an appropriate scaling variable.

We expect the approach outlined above, which consists in describing the probability distribution of  $\ln G$  by perturbative corrections to a log-normal form (thus characterized by only three quantities, namely, mean ( $\langle \ln G \rangle$ ), width [ $\Delta(\ln G)$ ], and skewness ( $S$ )) to be appropriate in the present

case of ferromagnetic disorder; it remains to be checked whether additional parameters, or even a change of perspective, will be necessary if frustration effects are present, e.g., in random-field [28] or spin-glass systems. We plan to undertake this task as a continuation of the present work.

#### ACKNOWLEDGMENTS

S.L.A.dQ. thanks the Department of Theoretical Physics at Oxford, where most of this work was carried out, for the hospitality, and the cooperation agreement between Academia Brasileira de Ciências and the Royal Society for funding his visit. Research of S.L.A.dQ. is partially supported by the Brazilian agencies Ministério da Ciência e Tecnologia, Conselho Nacional de Desenvolvimento Científico e Tecnológico, and Coordenação de Aperfeiçoamento de Pessoal de Ensino Superior.

- 
- [1] R. B. Stinchcombe, in *Phase Transitions and Critical Phenomena*, edited by C. Domb and J. L. Lebowitz (Academic, New York, 1983), Vol. 7.
- [2] B. N. Shalaev, Phys. Rep. **237**, 129 (1994).
- [3] W. Selke, L. N. Shchur, and A. L. Talapov, in *Annual Reviews of Computational Physics*, edited by D. Stauffer (World Scientific, Singapore, 1994), Vol. 1.
- [4] B. Derrida and H. Hilhorst, J. Phys. C **14**, L539 (1981).
- [5] B. Derrida, Phys. Rep. **103**, 29 (1984).
- [6] A. Crisanti, S. Nicolis, G. Paladin, and A. Vulpiani, J. Phys. A **23**, 3083 (1990).
- [7] A. Crisanti, G. Paladin, and A. Vulpiani, *Products of Random Matrices in Statistical Physics*, edited by Helmut K. Löttsch, Springer Series in Solid State Sciences Vol. 104 (Springer, Berlin, 1993).
- [8] R. B. Stinchcombe and B. P. Watson, J. Phys. C **9**, 3221 (1976).
- [9] A. P. Young and R. B. Stinchcombe, J. Phys. C **9**, 4419 (1976).
- [10] S. Wiseman and E. Domany, Phys. Rev. E **52**, 3469 (1995).
- [11] See, e.g., R. A. Hyman, Kun Yang, R. N. Bhatt, and S. M. Girvin, Phys. Rev. Lett. **76**, 839 (1996), and references therein.
- [12] M. E. Fisher, in *Critical Phenomena*, Proceedings of the International School of Physics "Enrico Fermi," Course LI, Varenna, 1970, edited by M. S. Green (Academic, New York, 1971).
- [13] M. N. Barber, in *Phase Transitions and Critical Phenomena*, edited by C. Domb and J. L. Lebowitz (Academic, New York, 1983), Vol. 8.
- [14] M. P. Nightingale, J. Appl. Phys. **53**, 7927 (1982).
- [15] M. P. Nightingale, in *Finite Size Scaling and Numerical Simulations of Statistical Systems*, edited by V. Privman (World Scientific, Singapore, 1990).
- [16] J. L. Cardy, in *Phase Transitions and Critical Phenomena*, edited by C. Domb and J. L. Lebowitz (Academic, New York, 1987), Vol. 11.
- [17] H.-F. Cheung and W. L. McMillan, J. Phys. C **16**, 7027 (1983); **16**, 7033 (1983); D. A. Huse and I. M. Morgenstern, Phys. Rev. B **32**, 3032 (1985); U. Glaus, *ibid.* **34**, 3203 (1986); J. Phys. A **20**, L595 (1987).
- [18] S. L. A. de Queiroz and R. B. Stinchcombe, Phys. Rev. B **46**, 6635 (1992); **50**, 9976 (1994).
- [19] S. L. A. de Queiroz, Phys. Rev. E **51**, 1030 (1995).
- [20] F. D. A. Aarão Reis, S. L. A. de Queiroz, and R. R. dos Santos (unpublished).
- [21] R. Fisch, J. Stat. Phys. **18**, 111 (1978).
- [22] W. Kinzel and E. Domany, Phys. Rev. B **23**, 3421 (1981).
- [23] A. L. Talapov and L. N. Shchur, Europhys. Lett. **27**, 193 (1994).
- [24] T. T. Wu, B. M. McCoy, C. A. Tracy, and E. Barouch, Phys. Rev. B **13**, 316 (1976).
- [25] R. Brout, Phys. Rev. **115**, 824 (1959).
- [26] A. W. W. Ludwig, Nucl. Phys. B **330**, 639 (1990).
- [27] W. Press, B. Flannery, S. Teukolsky, and W. Vetterling, *Numerical Recipes in Fortran, The Art of Scientific Computing*, 2nd ed. (Cambridge University Press, Cambridge, 1994).
- [28] E. D. Moore, R. B. Stinchcombe, and S. L. A. de Queiroz (unpublished).